vol. 173, no. 1 the american naturalist january 2009

E-Article

# Resource Patch Formation and Exploitation throughout the Marine Microbial Food Web

**J. R. Seymour,[1,*] Marcos,[2,†] and R. Stocker[1,‡]**

1. Ralph M. Parsons Laboratory, Department of Civil and Environmental Engineering, Massachusetts Institute of Technology, Cambridge, Massachusetts 02139;
2. Department of Mechanical Engineering, Massachusetts Institute of Technology, Cambridge, Massachusetts 02139

*Submitted January 23, 2008; Accepted May 23, 2008; Electronically published December 3, 2008*

abstract: Exploitation of microscale ($\mu$m–mm) resource patches by planktonic microorganisms may influence oceanic trophodynamics and nutrient cycling. However, examinations of microbial behavior within patchy microhabitats have been precluded by methodological limitations. We developed a microfluidic device to generate microscale resource patches at environmentally realistic spatiotemporal scales, and we examined the exploitation of these patches by marine microorganisms. We studied the foraging response of three sequential levels of the microbial food web: a phytoplankton (*Dunaliella tertiolecta*), a heterotrophic bacterium (*Pseudoalteromonas haloplanktis*), and a phagotrophic protist (*Neobodo designis*). Population-level chemotactic responses and single-cell swimming behaviors were quantified. *Dunaliella tertiolecta* accumulated within a patch of $NH_4^+$, simulating a zooplankton excretion, within 1 min of its formation. *Pseudoalteromonas haloplanktis* cells also exhibited a chemotactic response to patches of *D. tertiolecta* exudates within 30 s, whereas *N. designis* shifted swimming behavior in response to bacterial prey patches. Although they relied on different swimming strategies, all three organisms exhibited behaviors that permitted efficient and rapid exploitation of resource patches. These observations imply that microscale nutrient patchiness may subsequently trigger the sequential formation of patches of phytoplankton, heterotrophic bacteria, and protozoan predators in the ocean. Enhanced uptake and predation rates driven by patch exploitation could accelerate carbon flux through the microbial loop.

*Keywords:* phytoplankton, bacteria, flagellate, resource patch, chemotaxis, planktonic.

* Corresponding author; e-mail: justins@mit.edu.

† E-mail: acos@mit.edu.

‡ E-mail: romans@mit.edu.

Am. Nat. 2009. Vol. 173, pp. E15–E29. 
0003-0147/2009/17301-50213$15.00.
DOI: 10.1086/593004

Patchy distributions of resources and organisms occur in most natural habitats (Levin and Whitfield 1994). To succeed within heterogeneous environments, organisms must possess movement and search behaviors that maximize exposure to limiting resources (Grünbaum 1998). The ability to locate and exploit patches becomes particularly important in environments where background resource availability is low (Mullin and Brooks 1976; Leising and Franks 2000). This scenario is pertinent in the ocean, where planktonic microorganisms regularly experience background concentrations of limiting nutrients and prey that are below the critical limits required for optimum growth (Mullin and Brooks 1976; McCarthy and Goldman 1979). To understand how environmental heterogeneity affects the ecology of populations, it is imperative to explore foraging behavior at environmentally relevant spatiotemporal scales (Wiens 1989). For microbes in the upper ocean, these scales are often miniscule.

The ocean was once considered to be homogeneous at small scales (Hutchinson 1961) and is still widely modeled as uniform at scales of <1 m. However, there is substantial evidence that oceanic patchiness is pervasive at all scales (Haury et al. 1978), even down to the microscales ($\mu$m–mm) at which motility and perceptive distances of microorganisms operate (Azam 1998; Fenchel 2002; Azam and Malfatti 2007). Microscale patches of resources for planktonic microbes are predicted to originate from diverse ecological and physicochemical processes (Lehman and Scavia 1982*a*, 1982*b*; Mitchell et al. 1985; Blackburn et al. 1997, 1998; Kiørboe and Jackson 2001). Ephemeral micropatches, which are rich in dissolved inorganic nutrients (DIN), may support a large percentage of the phytoplankton production in otherwise oligotrophic waters (Goldman et al. 1979; McCarthy and Goldman 1979). Similarly, micropatches of dissolved organic carbon (DOC) are predicted to support hotspots of bacterial activity and growth (Azam 1998; Fenchel 2002). The capacity of planktonic microbes to actively locate and exploit these resource islands within a patchy milieu will therefore shape trophic

interactions within the microbial loop (Azam et al. 1983; Blackburn et al. 1997) and is predicted to enhance productivity levels and biogeochemical fluxes (Azam 1998; Blackburn and Fenchel 1999*a*; Azam and Long 2001). A detailed understanding of the foraging abilities of marine microbes within a heterogeneous seascape is therefore an important requisite to quantifying their effect on the ecology and biogeochemistry of the ocean.

Although some zooplankton exhibit behavioral adaptations that are tuned to heterogeneous prey distributions (Tiselius 1992; Leising 2001; Leising and Franks 2002; Menden-Deuer and Grünbaum 2006), swimming microbes have generally been considered to be too slow and insensitive to be able to exploit microscale resource patches in all but the most stable oceanic environments (Mitchell et al. 1985; Jackson 1987). However, increasing environmental (Seymour et al. 2000, 2004; Doubell et al. 2006), metabolic (Azam and Hodson 1981; Goldman and Gilbert 1982), behavioral (Mitchell et al. 1995, 1996; Blackburn et al. 1998; Barbara and Mitchell 2003*a*, 2003*b*), and genomic (Moran et al. 2004) evidence suggests that marine bacteria and phytoplankton may also be adapted to life in a patchy habitat. Detailed examinations of microbial foraging in patchy aquatic microhabitats have, so far, been limited by methodological constraints that have prevented the reproducible generation of controlled and realistic resource patches at submillimeter scales.

Recent advances in microfluidics (Whitesides et al. 2001; Weibel et al. 2007) have enabled detailed analyses of microbial ecology within complex microhabitats (Mao et al. 2003; Park et al. 2003; Keymer et al. 2006; Marcos and Stocker 2006). We utilized microfluidic technology to generate microscale resource patches and investigated how three model compartments of the oceans' planktonic food web, representing key players in the microbial loop (Azam et al. 1983), respond to a patchy habitat. This allowed us to quantify the temporal and spatial scales over which resource patches are exploited by microorganisms, which may be applied to predict the magnitude of rate transfer functions through the marine microbial food web.

## Methods

### *Generating Microscale Resource Patches Using a Microfluidic Channel*

A microfluidic channel was designed and fabricated for the purpose of generating a microscale resource patch with dimensions and dynamics consistent with those predicted to occur in the ocean (Jackson 1980; Blackburn et al. 1997, 1998). Soft lithographic techniques (Whitesides et al. 2001), described previously (Marcos and Stocker 2006; Seymour et al. 2007), were used to fabricate the microfluidic device (fig. 1*a*), which consisted of a 45-mm-long (working section of 25 mm), 3-mm-wide, and 50-$\mu$m-deep channel. Two inlet points were employed to separately inject organisms and substrates (or prey) into the channel at 240 $\mu$m $s^{-1}$ using a syringe pump (PHD2000, Harvard Apparatus, Holliston, MA). Inlet A led to a 100-$\mu$m-wide polydimethylsiloxane (PDMS) microinjector, which was used to generate a coherent band of nutrients or prey. This band distended to a width of 300 $\mu$m on injection into the main channel (fig. 1*b*). The concentration distribution was monitored directly by adding fluorescein to nutrient solutions (final concentration, 100 $\mu$M) before injection into the channel and visualizing fluorescence intensities using epifluorescence microscopy. Organisms were injected via inlet B, upstream of the nutrient injection point, and were advected along both sides of the nutrient band until the syringe pump was stopped (time, $t = 0$). This caused all flow in the channel to stop instantaneously, as inertia is negligible at the small Reynolds number (~0.01) that is characteristic of flow within the channel. The nutrient band then began to diffuse laterally, simulating a pulse release of nutrients.

### *Response of Phytoplankton to Microscale Nutrient Patches*

We first examined whether the motile marine phytoplankton *Dunaliella tertiolecta* is capable of exploiting localized patches of inorganic nutrients modeled on those predicted to arise from zooplankton excretions (McCarthy and

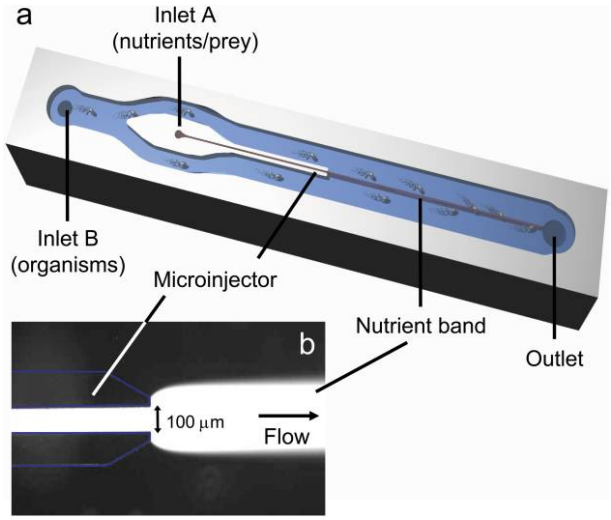


**Figure 1:** *a*, Schematic diagram of the microfluidic channel. Channel width and depth are 3 mm and 50 $\mu$m, respectively. Nutrients and organisms were injected separately, via inlets A and B, using a syringe pump. *b*, Fluorescent microscope image (20×) showing injection of a nutrient band, visualized by adding 100 $\mu$M fluorescein dye.

Goldman 1979; Lehman and Scavia 1982*a*, 1982*b*). Axenic cultures of *D. tertiolecta* (CCMP1320) were grown in f/20 growth medium (Guillard and Ryther 1962) under constant light conditions to early exponential growth stage, equating to a mean cell density of $\sim 2 \times 10^4$ cells $mL^{-1}$. Cells were centrifuged at 500 *g* for 5 min and the pellet was washed and resuspended in artificial seawater (ASW; NaCl [400 mM], $CaCl_2 \cdot 2H_2O$ [10 mM], KBr [1.7 mM], KCl [10 mM], $MgCl_2 \cdot 6H_2O$ [20 mM], and $MgSO_4 \cdot 7H_2O$ [20 mM]). The washed cells were then deprived of nutrients ("starved") for 12 h before being washed again in ASW immediately before the experiments.

The chemotactic response of *D. tertiolecta* cells to a microscale patch of ammonium was examined by preparing $NH_4Cl$ in ASW in final concentrations of 0 (control), 5, 10, 50, 100, and 1,000 $\mu$M. A band of $NH_4Cl$ was injected into the channel as described above, and the response of *D. tertiolecta* was measured by videomicroscopy (see below). To determine the relative nutrient advantage obtained by *D. tertiolecta* from chemotactic swimming in comparison with a nonmotile or nonchemotactic population, we integrated the nutrient exposure over the population using the measured cell distribution and nutrient concentration distribution, and we normalized this to the value calculated for an equally sized, theoretical population of nonswimming cells distributed uniformly across the channel width (Stocker et al. 2008).

### *Response of Bacteria to Microscale Phytoplankton Patches*

To determine the trophic consequences of the formation of a localized phytoplankton patch, we examined the chemotactic behavior of heterotrophic bacteria exposed to a patch of phytoplankton extracellular exudates. Cultures of the marine $\gamma$-proteobacteria *Pseudoalteromonas haloplanktis* (ATCC700530) were grown overnight in 1% Tryptic Soy Broth (TSB; Difco) supplemented with NaCl (400 mM), at room temperature, while being agitated on a shaker (175 rpm). Cultures were then diluted 1 : 20 in ASW before being starved at room temperature for 72 h (modified from Mitchell et al. 1996). Cultures were further diluted to $\sim 10^7$ cells $mL^{-1}$ so that individual bacteria could be unambiguously tracked over time.

In order to discriminate *P. haloplanktis* swimming trajectories without interference from phytoplankton cells or detritus, and in line with predictions that bacteria exhibit chemotaxis toward the dissolved organic matter exuded by phytoplankton (Azam and Ammerman 1984), a solution of the extracellular exudates obtained from cultures of *D. tertiolecta* was employed as the patch constituent here. *Dunaliella tertiolecta* culture filtrates (exudates) were obtained using the procedure of Bell and Mitchell (1972). To ensure that the f/2 algal growth medium present in the culture filtrate did not invoke a chemotactic response by *P. haloplanktis*, control experiments were conducted using sterile f/2 medium.

### *Response of Bacterivores to Microscale Bacteria Patches*

We next considered how hotspots of chemotactic bacteria might represent localized food patches for bacterivorous protozoan flagellates. Cultures of the heterotrophic flagellate *Neobodo designis* (CCAP1951/1) were grown in Plymouth Erdschreiber medium supplemented with wheat grains. Prior to experiments, a mid-exponential growth phase *P. haloplanktis* culture was added to the *N. designis* culture in a final concentration of 5% (vol/vol). *Neobodo designis* numbers were then allowed to increase for 3 days until near exhaustion of bacterial cells from the culture medium.

The response of *N. designis* to a patch of bacteria was investigated by injecting a band of *P. haloplanktis* cells into the microchannel via inlet A. *Pseudoalteromonas haloplanktis* cells were grown to the exponential growth phase. To inhibit motility of prey cells, thereby allowing maintenance of prey patch dimensions by preventing diffusion via random bacterial motility, *P. haloplanktis* cells were centrifuged at 10,000 *g* for 5 min to shear off flagella. The absence of motility was confirmed by microscopy. Cells were then resuspended in ASW in a final concentration of $\sim 10^7$ cells $mL^{-1}$, corresponding to a bacterial hotspot where cell numbers are 10-fold above typical oceanic background concentrations, which is consistent with previous predictions (Bowen et al. 1993; Blackburn and Fenchel 1999*a*) and direct observations (Blackburn et al. 1998). In line with the predicted duration of microscale hotspots of bacteria in the ocean (Blackburn et al. 1997, 1998), the response of *N. designis* to this prey patch was then measured for 13 min. Control experiments were performed where bacteria-free TSB medium was injected via inlet A.

### *Imaging and Analysis of Swimming Behavior*

Experiments were conducted using an inverted microscope (Eclipse TE2000-E, Nikon, Japan). The concentration of the nutrient patch was viewed and recorded throughout each experiment with epifluorescence imaging of the fluorescein concentration using an EXFO X-Cite 120 fluorescent lamp (EXFO Photonic Solutions, Ontario, Canada). The patch width was defined as the standard deviation of the concentration profile. The concentration profile of nutrients was assumed to correspond to that of fluorescein because the diffusion coefficient of fluorescein is very similar to that of low-molecular-weight organic substrates ($\sim 0.5 \times 10^{-9}$ $m^2$ $s^{-1}$). Organisms were observed at mid-

depth in the channel, 3 mm downstream of the nutrient injection point, using phase-contrast microscopy.

The experiment was initiated by stopping flow in the channel (time, $t = 0$), and measurements of fluorescence intensity and organism distributions were subsequently recorded at intervals of 0.5–2 min for at least 10 min. The positions and swimming paths of individual cells were obtained by recording sequences of 200–400 frames ("movies") at 10–32.4 frames per second, using a 1,600 × 1,200-pixel CCD camera (PCO 1600, Cooke, Romulus, MI). In-house-developed cell-tracking software (BacTrack) was employed to obtain bacterial trajectories, from which swimming statistics were calculated using Matlab (MathWorks, Natick, MA). Spatial maps of swimming statistics were obtained by binning data across the channel width into seven 430-$\mu$m-wide bins.

Mean swimming speeds ($u$) were calculated from cell displacements between consecutive frames. For *D. tertiolecta* and *P. haloplanktis*, we computed mean turning frequencies, where turns were operationally defined as changes in direction larger than 90°. This arbitrary definition of a turn serves the purpose of allowing a relative comparison among different conditions within a given population. The distance covered along a swimming path between two consecutive turns was defined as the run length ($\lambda$).

To gain further insight into the chemotactic behavior of *D. tertiolecta* and *P. haloplanktis* as they responded to nutrient patches, we calculated the chemotactic velocity ($v_c$) of each population, which is defined as the average velocity of migration up a chemical gradient. This can be computed as $v_c = u(1 - \beta)/(1 + \beta)$, where $\beta$ is the swimming direction asymmetry, defined as $\beta = \tau^-/\tau^+$, and $\tau^+$ and $\tau^-$ are the mean run times up and down the chemoattractant gradient, respectively (Rivero et al. 1989). Here we determined the chemotactic velocity by calculating $\beta$, obtained by measuring the ratio of the total time cells spent swimming away from and toward the center of the patch, respectively.

For *N. designis*, which swam in continuously curved paths, discrete runs and turns could not be defined, so changes in swimming behavior were instead measured by quantifying the net-to-gross displacement ratio (NGDR). The NGDR is defined as NGDR = ND/GD (Buskey 1984), where ND is the net displacement of a trajectory, or the straight-line distance between its start and end points, and GD is the gross displacement, or the total length of the trajectory. The NGDR is a measure of tortuosity, with NDGR → 1 corresponding to nearly straight trajectories and NDGR → 0 indicating increasingly convoluted trajectories. For each population, we used $t$-tests to compare mean swimming parameters between control and experimental conditions and within and outside of resource patches.

To relate measured swimming parameters to distributional patterns and to gain a more detailed insight into how behavior permits exploitation of resource patches, we developed two numerical models. The first was an individual-based model (IBM) designed to understand the role of spatial heterogeneity in swimming parameters in determining cell distributions. The second was a continuum model predicting the spatiotemporal accumulation patterns of a population of organisms parameterized using the swimming behaviors observed in the experiments. A detailed description of each model and its implementation is given in the appendix.

## Results

### *Generating Patches*

Highly reproducible patches of nutrients were generated using the microfluidic channel. After the flow was stopped, advective transport of organisms and nutrients ceased and patches began to spread laterally at a rate set by molecular diffusion, expanding to a width of 2.5 mm after $t = 5$ min (fig. 2). At $t = 5$ and 15 min, the mean nutrient concentration at the center of the patch (the central 300 $\mu$m) had decreased to 21% and 12% of the initial concentration, respectively.

### *Response of Phytoplankton to Microscale Nutrient Patches*

In the absence of nutrient patches, *Dunaliella tertiolecta* exhibited swimming patterns characterized by a mean swimming speed $u = 38 \pm 3$ $\mu$m s$^{-1}$ (mean ± SD;

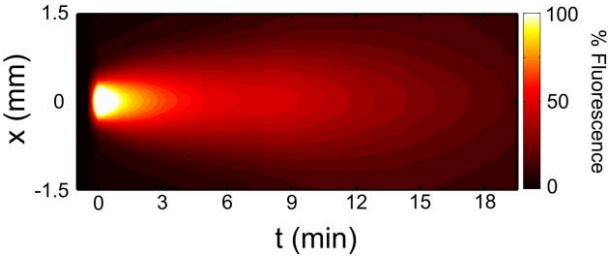


**Figure 2:** Spatiotemporal evolution of the nutrient band. The vertical axis represents position across the channel width, with $x = 0$ corresponding to midchannel (i.e., the center of the nutrient band). The horizontal axis corresponds to time elapsed after flow in the channel was stopped ($t = 0$), "releasing" the nutrient band. Data were compiled from 40 measurements taken at 30-s intervals at $y = 3$ mm downstream of the injection point. The scale bar represents relative fluorescence intensity of fluorescein dye, as a percentage of its initial value in the center of the patch ($x = 0$, $t = 0$).

$n = 63$ movies) and relatively straight runs periodically intersected by changes in direction, leading to a random dispersal of cells (fig. 3*a*). When a band of $NH_4^+$ was added to the center of the channel (fig. 3*b*), a rapid chemotactic response was observed, with cells aggregating strongly inside the nutrient band (fig. 3*c*) in <1 min. Accumulation of *D. tertiolecta* cells led to the formation of coherent, 600–800-$\mu$m-wide patches of phytoplankton, where cell numbers reached up to seven times background levels (fig. 4). These localized phytoplankton patches persisted for up to 7 min and were apparent for $NH_4^+$ concentrations ranging

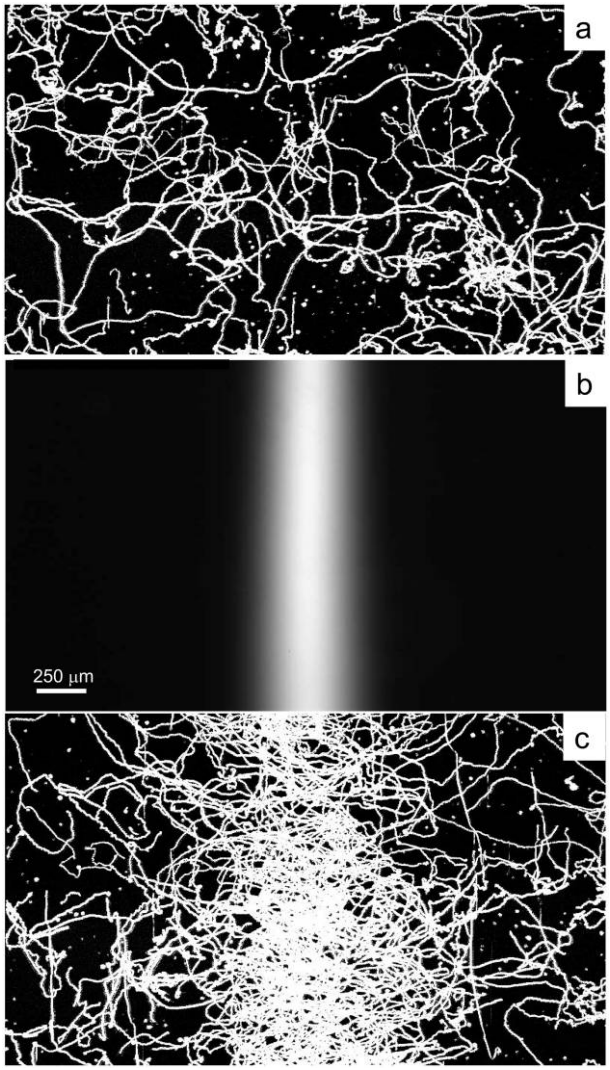


**Figure 3:** Swimming patterns of the phytoplankton *Dunaliella tertiolecta*. Each white path corresponds to a single trajectory. *a*, Trajectories in the absence of a nutrient patch. *b*, Initial position of a band of $NH_4^+$, visualized with 100 $\mu$M fluorescein. *c*, Trajectories recorded at $t = 2$ min showing strong aggregation of cells in the nutrient patch. In both *a* and *c*, trajectories were recorded over 40 s at 10 frames $s^{-1}$.

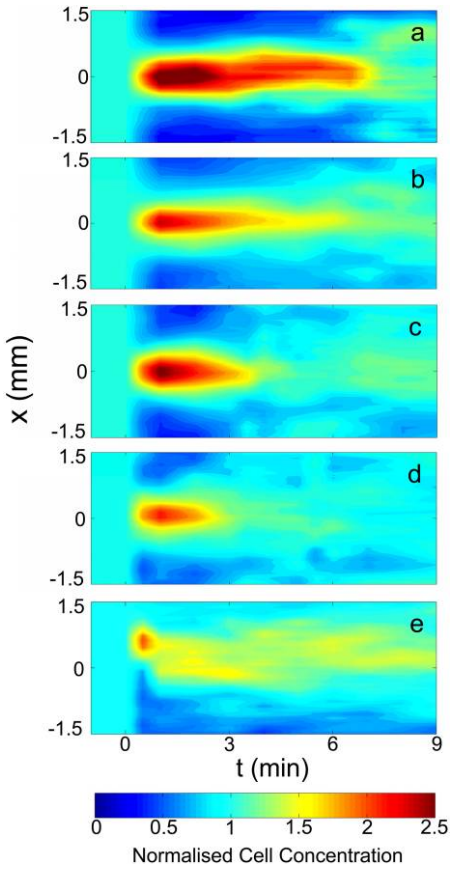


**Figure 4:** Spatiotemporal maps of the phytoplankton *Dunaliella tertiolecta* distribution, recorded at 1-min intervals (normalized to a mean of 1), following the addition of $NH_4^+$ patches of varying concentration: (*a*) 1 mM, (*b*) 100 $\mu$M, (*c*) 50 $\mu$M, (*d*) 10 $\mu$M, (*e*) 5 $\mu$M. Axes as in figure 2.

from 1 mM down to 5 $\mu$M (fig. 4), with their intensity and duration varying with $NH_4^+$ concentration. This chemotactic response gave *D. tertiolecta* up to a 230% advantage in nutrient exposure over a theoretical population of nonswimming cells in the case of a 1-mM patch.

Accumulation of cells within the nutrient patch was accompanied by changes in swimming behavior. While we observed no significant shift in swimming speed irrespective of nutrient concentration or position in the patch, turning frequencies varied significantly in response to the patch. In the central 430 $\mu$m of the channel, corresponding to the center of the nutrient patch, mean turning frequencies ($f = 1.4 \pm 0.1$ Hz) were significantly ($P < .05$) diminished compared with those outside of the patch ($f = 2.0 \pm 0.1$ Hz). This pattern persisted for the entire period during which *D. tertiolecta* cells remained aggregated inside the nutrient patch. During this time, the chemotactic velocity $v_c$ was 5.2 $\mu$m $s^{-1}$, or 14% of $u$. Control

experiments, where a band of ASW was injected instead of a band of nutrients, resulted in neither aggregation nor observable changes in swimming behavior.

### *Chemotactic Response of Bacteria to Microscale Phytoplankton Patches*

When suspended in ASW under uniform nutrient conditions, *Pseudoalteromonas haloplanktis* cells swam with a mean speed $u = 57 \pm 2$ $\mu$m s$^{-1}$ ($n = 50$ movies), reaching bursts of 438 $\mu$m s$^{-1}$. The average turning frequency was $f = 4.1 \pm 1.1$ Hz, the inverse of this corresponding to a mean run duration $\tau = 0.24 \pm 0.08$ s, which led to a mean run length $\lambda = 14 \pm 2$ $\mu$m ($n = 50$). Inspection of trajectories revealed that turns were often reversals rather than random reorientations, which is in agreement with previous observations for this species (Barbara and Mitchell 2003*b*).

In the presence of a band of *D. tertiolecta* extracellular exudates, *P. haloplanktis* cells exhibited rapid and strong aggregation. A clear and intense band of bacteria, corresponding to the initial position of the nutrient patch, formed in <30 s, with cell numbers within the patch reaching more than eight times background levels (fig. 5). The band of bacteria gradually spread as the nutrient patch diffused, but a clear aggregation of cells persisted for almost 20 min (fig. 6*a*).

The swimming behaviors of *P. haloplanktis* cells changed substantially in response to the nutrient patch. Mean swimming speeds within the patch increased by 23%, reaching 70 $\mu$m s$^{-1}$. Elevated swimming speeds persisted for at least 20 min, and as the patch diffused laterally, speeds progressively increased across the entire channel width (fig. 6*b*). Turning frequencies and run lengths also changed in response to the nutrient patch. Mean turning frequencies increased significantly ($P < .05$) to $f = 6.9 \pm 0.9$ Hz, with $\tau = 0.15 \pm 0.02$ s, and mean run lengths decreased to $\lambda = 9.1 \pm 1.9$ $\mu$m ($n = 50$ movies). A clear spatiotemporal pattern in the mean turning frequency was also evident (fig. 6*c*), with significantly ($P < .05$) higher values found at the edges of the nutrient patch ($f = 8.0 \pm 0.8$ Hz; $\tau = 0.12 \pm 0.01$ s; $\lambda = 7.5 \pm 0.8$ $\mu$m; $n = 35$) than within the central, high-nutrient region ($f = 5.5 \pm 0.6$ Hz; $\tau = 0.19 \pm 0.02$ s; $\lambda = 12.5 \pm 0.9$ $\mu$m; $n = 10$). During the first 8.5 min, $v_c = 5.0$ $\mu$m s$^{-1}$, corresponding to 9% of $u$. Control experiments, wherein a band of ASW was injected, resulted in neither aggregation nor observable changes in swimming behavior ($P > .05$).

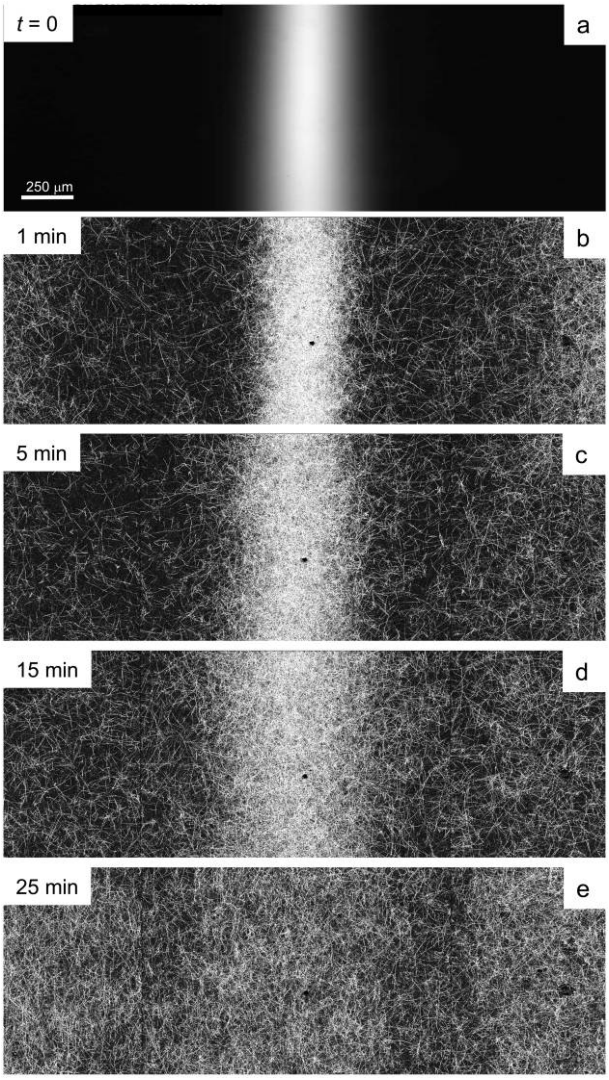


**Figure 5:** Aggregation of *Pseudoalteromonas haloplanktis* bacteria in a band of *Dunaliella tertiolecta* exudates. *a*, Initial position of the exudate band. *b*, *Pseudoalteromonas haloplanktis* trajectories $t = 1$ min after patch release. *c*, $t = 5$ min. *d*, $t = 15$ min. *e*, $t = 25$ min. In each case, trajectories were recorded over 9.3 s at 32.4 frames s$^{-1}$.

### *Response of Bacterivores to Microscale Bacteria Patches*

A bacterial patch was created by injecting a layer of *P. haloplanktis* in lieu of a chemical attractant, and the response of the heterotrophic flagellate *Neobodo designis* was examined. Like other planktonic protists (Fenchel and Blackburn 1999), the swimming behavior of *N. designis* is characterized by a rotation around the cells' longitudinal axes (Lee et al. 2005), which generates helical swimming trajectories composed of both a translational and a rotational component (Crenshaw 1996; fig. 7*a*). Under homogeneous, low-prey conditions, *N. designis* swam at

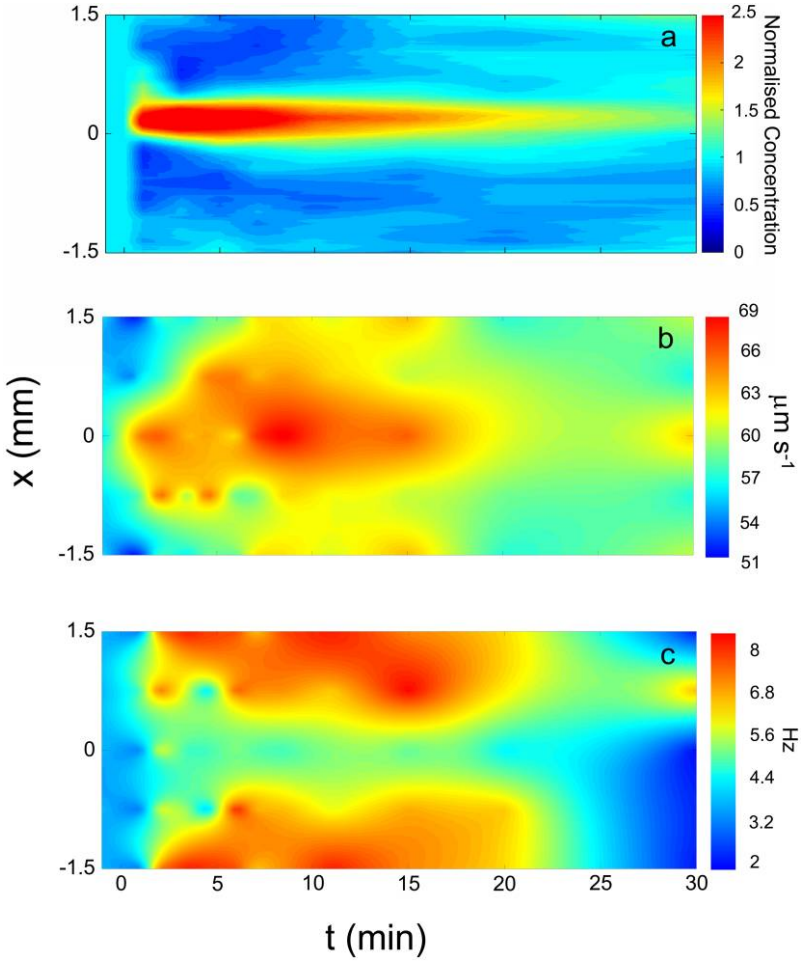


**Figure 6:** Spatiotemporal distributions and changes in swimming statistics of *Pseudoalteromonas haloplanktis* bacteria following addition of a patch of *Dunaliella tertiolecta* exudates. Axes as in figure 2. *a*, Relative concentration of *P. haloplanktis* cells, normalized to a mean of 1. *b*, Swimming speed *u*. *c*, Turning frequency *f*.

69 ± 6 $\mu$m s$^{-1}$ in relatively straight translational trajectories, with rare changes in direction (fig. 7*a*). This was reflected by high NGDR values (0.75 ± 0.15; $n = 6$ movies) and allowed individual cells to rapidly explore the entire channel width. After exposure to a band of bacteria, the swimming behavior of *N. designis* changed markedly. Mean swimming speeds were significantly ($P < .05$) lower (58 ± 6 $\mu$m s$^{-1}$; $n = 12$) than in the homogeneous prey conditions and typically decreased with time of exposure to the patch (fig. 7). Trajectories also became significantly ($P < .05$) more tortuous and remained so for 13 min, enabling individual cells to maintain close association with the position of the prey patch (fig. 7). This increase in tortuosity was confirmed by a strong decrease in NGDR, with a mean NGDR of 0.36 ± 0.09 ($n = 12$) observed for all trajectories during the time of exposure to the bacterial patch (13 min) and values as low as 0.24 observed 5 min after initial patch exposure. In control experiments where ASW was injected into the channel, no shifts in swimming behavior were observed.

## Discussion

We measured the behavioral responses of swimming microorganisms to microscale resource patches that are predicted to occur in the ocean (Lehman and Scavia 1982*a*, 1982*b*; Blackburn et al. 1997, 1998; Azam 1998; Kiørboe and Jackson 2001; Fenchel 2002). The underlying behavior allowing microbes to exploit patches at these scales is chemotaxis. Chemotaxis is typically assessed using the capillary assay method (Adler 1969), which, while providing information about the sensitivity of microbes to a given

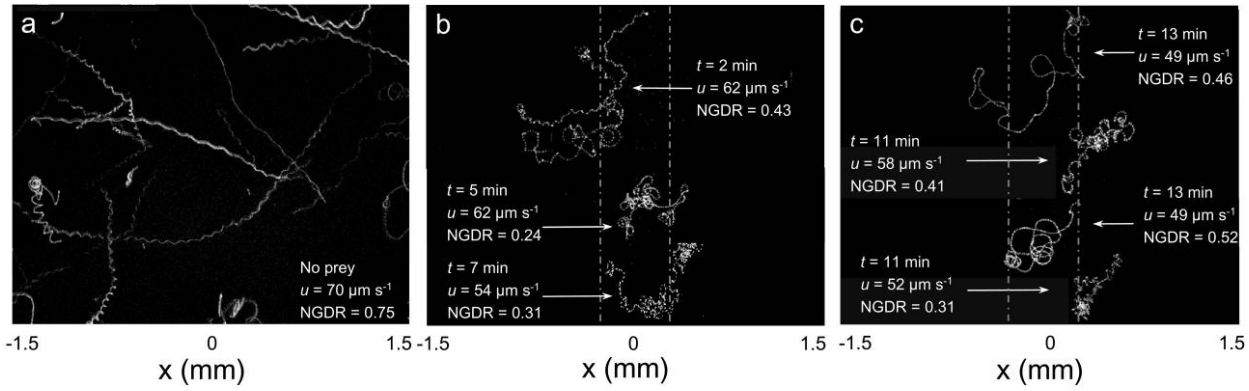


**Figure 7:** Representative trajectories of the heterotrophic flagellate *Neobodo designis* exposed to a prey patch composed of *Pseudoalteromonas haloplanktis* bacteria. *a*, Control case (no prey), recorded over 40 s. *b*, *c*, Trajectories at different times *t* after release of the patch. Values of swimming speed *u* and net-to-gross displacement ratio (*NGDR*) are indicated (mean values shown for the control case). Dotted lines represent approximate boundaries of bacterial prey patches. In all cases, trajectories were recorded at 10 frames $s^{-1}$.

chemical, does not allow direct observation of organism behavior within a spatially complex habitat. Microfluidic devices such as the one presented here can, however, be used to produce coherent patches at micrometer to millimeter scales, enabling detailed examination of microbial foraging behavior within a heterogeneous microenvironment.

In the ocean, mixing by turbulence becomes negligible at scales below the Kolmogorov scale (Lazier and Mann 1989), which is typically 1–30 mm (Mitchell et al. 1985). Thus, at the spatial scales of the patches considered here, the erosive influence of molecular diffusion is the primary physical factor restricting the time frame of patch availability. Our microfluidic system enabled the generation of purely diffusive resource patches with lifetimes and dimensions commensurate with patches predicted to occur in the ocean.

### *Exploitation of Nutrient Patches by Phytoplankton*

A long-standing oceanographic hypothesis predicts that phytoplankton in oligotrophic habitats may obtain an important fraction of their nutrient requirements from transient exposure to microscale nutrient patches produced by zooplankton excretions (Goldman et al. 1979; McCarthy and Goldman 1979; Goldman and Gilbert 1982; Lehman and Scavia 1982*a*, 1982*b*). Conversely, it has been argued that such patches will diffuse too rapidly and that the time spent in a patch will be too short to have a significant effect on phytoplankton production (Jackson 1980; Williams and Muir 1981). However, only phytoplankton uptake and patch dissipation rates have been considered within this context, whereas the potential roles of motility and chemotaxis in exploiting patches have been largely overlooked. Although phytoplankton chemotaxis toward some organic and inorganic substrates has been demonstrated (Sjoblad and Frederikse 1981; Kohidai et al. 1996; Lee et al. 1999), the spatiotemporal scales of the response and the magnitude of the resulting aggregation have never been investigated experimentally.

The microchannel applied here generated diffusing nutrient patches with dimensions comparable to the predicted chemical trail behind a swimming zooplankter (Jackson 1980) or the wake of a sinking marine snow particle (Kiørboe and Jackson 2001). The ammonium concentrations eliciting a chemotactic response in our experiments (5 $\mu$M–1 mM) are also realistic when compared with those expected in a zooplankton excretion (~5 $\mu$M; McCarthy and Goldman 1979; Jackson 1980) or associated with marine snow particles (up to 8 mM; Prezelin and Alldredge 1983). Nutrient patches occurring in the trails of zooplankton or sinking particles may extend several centimeters (Lehman and Scavia 1982*a*; Kiørboe and Jackson 2001) and persist for up to 10–15 min (Kiørboe and Jackson 2001). The strong and rapid chemotactic accumulation of *Dunaliella tertiolecta* observed here indicates that some motile phytoplankton are capable of aggregating inside nutrient patches in <1 min. Therefore, rather than gaining only passive exposure to nutrient-enriched patches, some phytoplankton are clearly capable of actively locating and exploiting patches within the time limits set by diffusion.

*Dunaliella tertiolecta* cells responded to nutrient patches by altering turning frequencies according to position within the nutrient gradient. *Dunaliella* species cells are propelled by two symmetrical anterior flagella, and changes in swimming direction, or "tumbles," occur when one of them temporarily stops beating (Schoevaert et al.

1988). The frequency of these tumbles ($f$) was 22% lower inside the nutrient patch compared with the outside of the patch. This is indicative of a chemotactic behavior, or a biased random walk, where cells swimming up a nutrient gradient decrease $f$ (i.e., increase $\tau$), resulting in net migration of cells up the gradient (Berg 1993). Whereas decreased $f$ will drive faster migration rates up a gradient, this also leads to a higher diffusivity of a random walking population, where $D = u^2/f$ (Berg 1993). Within a patch scenario, elevated $D$ inside the patch could potentially cause cells to swim out of the patch rather than to accumulate within the high nutrient central region of the patch. However, for a chemotactic population, shifts in $f$ are strongly biased according to whether a cell is swimming into or out of the center of the patch (Mittal et al. 2003). This bias ultimately drives a positive chemotactic velocity $v_c$ of a population (Rivero et al. 1989), as we observed here for *D. tertiolecta*. The relative magnitude of $v_c$ observed here ($v_c/u \sim 14\%$) is highly comparable with that observed for other chemotactic microbes (Berg and Brown 1972; Dahlquist et al. 1976) and resulted in the accumulation of *D. tertiolecta* cells within the center of the nutrient patch, which is consistent with the predictions of our IBM simulation (see appendix).

When parameterized using the measured swimming statistics from our experiments, the continuum model also predicted accumulation dynamics that were highly compatible with the observed patterns (see fig. 8*a* and appendix). In particular, the model correctly captured the rapid initial accumulation of cells, its width, and its peak magnitude (~2.5). Although dissipation of the cell aggregation occurs more slowly in the numerical simulations than in experiments, the consistency of the initial accumulation dynamics in the model supports our conclusion that the observed chemotactic swimming behavior is responsible for triggering the rapid and intense clustering of cells within nutrient patches.

Although swimming is widespread among phytoplankton (Horner et al. 1997), its ecological importance has typically been considered primarily in relation to photic migration (Kamykowski et al. 1998), physical stratification (Erga et al. 2003), or sex (Govoronova and Sineshchekov 2005). Our observations indicate that phytoplankton motility and chemotaxis can significantly increase exposure to nutrient patches, imparting a considerable nutrient advantage to chemotactic cells.

### *Chemotactic Response of Bacteria to Microscale Phytoplankton Patches*

Localized and ephemeral aggregations of phytoplankton, such as those observed in our study, may represent important growth habitats for heterotrophic bacteria. Within aquatic habitats, the ecology of heterotrophic bacteria is intimately linked to phytoplankton abundance and production across multiple scales (Cole 1982). At the smallest scales of interaction, bacteria may experience enhanced nutrient exposure by exploiting the microzone of organic exudates emanating from individual phytoplankton cells (Azam and Ammerman 1984; Mitchell et al. 1985; Bowen et al. 1993). Marine bacteria have even been shown to actively "chase" swimming phytoplankton cells (Barbara and Mitchell 2003*a*). Any aggregative behavior of phytoplankton may enhance this effect by increasing the concentration of phytoplankton-derived DOC within a patch (Rothschild et al. 1999). We examined this by presenting the marine bacterium *Pseudoalteromonas haloplanktis* with a patch composed of the extracellular products of *D. tertiolecta*. The strong chemotactic response demonstrated by *P. haloplanktis* resulted in an intense aggregation of cells inside the patch in <1 min, well within the lifetime of the phytoplankton aggregations observed above. Because patchiness of phytoplankton occurs across these scales in situ (Doubell et al. 2006), behavioral responses such as these are probably an important element in phytoplankton-bacteria interactions in the ocean.

The relatively high swimming speeds and "run-reverse" swimming strategy exhibited by *P. haloplanktis* are common among marine bacteria (Mitchell et al. 1995, 1996; Johansen et al. 2002; Barbara and Mitchell 2003*a*, 2003*b*) and have been proposed to be advantageous for maintaining position near point sources of nutrients in the ocean (Barbara and Mitchell 2003*b*; Thar and Fenchel 2005). As well as these adaptations, *P. haloplanktis* cells exhibited two clear behavioral shifts in response to patches. Bacteria inside the patch (1) swam 23% faster and (2) experienced an increase in turning frequency of 63%, with highest turning rates at the boundaries of the patch. Maximum turning frequencies at patch boundaries, coupled with positive chemotactic velocities, are consistent with bacterial chemotaxis and prevent cells from leaving high-nutrient regions (Mittal et al. 2003). The observed shifts in speed and turning rates are also similar to the behavior of marine bacteria clustering at oxic interfaces (Mitchell et al. 1995, 1996), but are in contrast with (1) area-restricted searching strategies, where slowing down inside patches is most advantageous (Benhamou 1992), and (2) the classical description of bacterial chemotaxis developed for *Escherichia coli* (Berg 1993), where cells swimming up a nutrient gradient maintain a constant swimming speed (Brown and Berg 1974). The increases in speed observed here are consistent with previous observations of *P. haloplanktis* cells increasing speed when exposed to amino acids (Barbara and Mitchell 2003*b*) and are characteristic of a nondirectional chemokinetic response, where bacteria increase swimming speed in response to a local stimulus

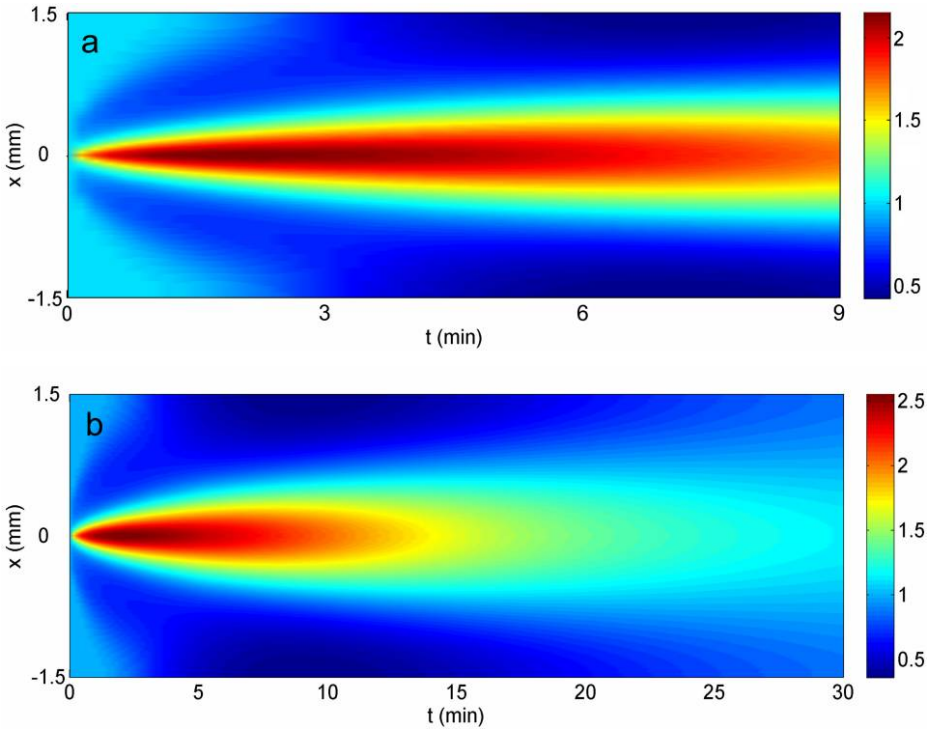


**Figure 8:** Spatiotemporal accumulation patterns of *Dunaliella tertiolecta* (*a*) and *Pseudoalteromonas haloplanktis* (*b*) as predicted by the continuum model, using observed values of the swimming parameters for each population (see appendix for details). Axes as in figure 2.

(Zhulin and Armitage 1993; Packer and Armitage 1994; D'Orsogna et al. 2003). The mechanism driving bacterial chemokinesis is not clear, but enhanced metabolism may be responsible for increasing the electrochemical proton gradient, driving higher rates of flagellar rotation (Zhulin and Armitage 1993).

Behavioral changes of this nature directly affect the dispersion and chemotaxis properties of a bacterial population. A large swimming speed $u$ may be advantageous for exploiting moving or diffusing nutrient sources in the ocean (Mitchell et al. 1996; Kiørboe and Jackson 2001; Barbara and Mitchell 2003*a*, 2003*b*) and will also act to increase the chemotactic velocity (migration rate) $v_c$ toward an attractant (Rivero et al. 1989). However, higher $u$ will also increase random motility $\mu = u^2\tau/3$ (Lovely and Dahlquist 1975) and hence will reduce the ability of bacteria to tightly cluster at point sources (Packer and Armitage 1994). This dispersive effect can be counteracted by a decrease in the mean run time $\tau$. Indeed, we observed a 38% decrease in $\tau$ (from 0.24 to 0.15 s) for bacteria associated with patches, nearly compensating for the 51% increase in $u^2$ in the expression for $\mu$. Similar decreases in $\tau$ (threefold) and increases in $u$ (twofold) have also been observed when *P. haloplanktis* cells track swimming phytoplankton (Barbara and Mitchell 2003*a*). As with *D. tertiolecta*, when parameterized using these measured swimming statistics, the continuum model yielded accumulation patterns in good agreement with those observed for *P. haloplanktis* in the experiments (fig. 8*b*; appendix). Although fast swimming is advantageous for chemotaxis in the ocean (Kiørboe and Jackson 2001; Barbara and Mitchell 2003*a*, 1991*b*), the quadratic scaling of energy consumption with swimming speed (Mitchell 1991) may prohibit continuous high-speed swimming. Therefore, *P. haloplanktis* may respond chemokinetically to an initial nutrient stimulus by upshifting speed to reach high-concentration regions more rapidly.

These observations indicate that some marine bacteria exhibit specialized behavioral adaptations that permit the rapid and efficient location and exploitation of patches of phytoplankton-derived DOM. We have previously shown that this behavior can afford up to a 10-fold gain in nutrient exposure to chemotactic bacteria (Stocker et al. 2008). Theoretical predictions also link bacterial chemotaxis in the ocean to significant increases in bacterial growth rates (Kiørboe and Jackson 2001) and a doubling of DOM remineralization rates (Blackburn et al. 1998; Fenchel 2002). Our observations provide strong experi-

mental support for the behavioral elements of these predictions.

### *Localized Predation on Patches of Bacteria*

Our experiments indicate that microscale bacterial patches, such as those observed here (fig. 5) and in situ (Seymour et al. 2004), may represent localized food sources for heterotrophic flagellates. Predation by bacterivores is a major cause of bacterial mortality in the ocean (Sherr and Sherr 2002) and is the principal link between the microbial food web and higher trophic levels (Azam et al. 1983). Phagotrophic protists exhibit chemotactic responses to the chemical products of bacteria (Sibbald et al. 1987) and may sense the chemical cloud surrounding a microscale patch of bacteria (Fenchel and Jonsson 1988; Blackburn and Fenchel 1999*b*). Experimental (Fenchel and Jonsson 1988; Fenchel and Blackburn 1999) and numerical (Blackburn and Fenchel 1999*b*) evidence indicates that some protists can exploit point sources of food by altering swimming behavior. We found that *Neobodo designis* cells homed in on prey patches within 2 min of their formation, indicating that bacterivores respond sufficiently rapidly to exploit bacterial hotspots within typical patch lifetimes in the ocean.

Behavioral shifts are imperative for predators to gain from heterogeneous prey distributions (Nachman 2006). When exposed to prey patches, *N. designis* cells exhibited more convoluted swimming patterns, characterized by significantly lower NGDR values, enabling them to remain within the vicinity of the prey patch. Unlike the swimming patterns of *D. tertiolecta* and *P. haloplanktis*, this maneuvering behavior is in line with area-restricted foraging (Benhamou 1992). The chemosensory swimming behavior of *N. designis* also exhibited characteristics consistent with helical klinotaxis, where cells swimming along a helical path are able to "steer" in gradients and orient directly to a chemical stimulus, without a biased random walk (Crenshaw 1993, Fenchel and Blackburn 1999). These observations confirm that microscale aggregations of bacteria in the ocean can become localized food patches for bacterivorous protozoa, potentially increasing predation rates and leading to an enhanced transfer of microbial biomass into the higher planktonic food web (Azam et al. 1983).

## Conclusions

Within heterogeneous landscapes, patchiness of resources creates complexity at multiple scales, influencing the dispersal and behavior of foragers (Levin and Whitfield 1994) and potentially either increasing (Rovinsky et al. 1997; Brentnall et al. 2003) or decreasing (Gao et al. 2004) the productivity of populations and ecosystems. Central to any question regarding the ecological importance of habitat patchiness is organism behavior or, more specifically, the extent to which foragers are able to modify behavior in response to nonuniform resource distribution. Although the ocean is now predicted to be patchy down to the scales of microbial interactions ($\mu$m–mm; Azam 1998; Fenchel 2002), our current perception of microbial ecology and behavior within a heterogeneous microhabitat is still rudimentary. The results presented here indicate that diverse populations of marine microbes can markedly modify their foraging behavior when navigating a patchy habitat, enabling rapid and efficient exploitation of short-lived resource patches. Because of technical complexities associated with tracking multiple populations of microbes simultaneously, we studied the foraging behavior of each organism separately. However, provided the observed behavioral responses co-occur in the ocean, we propose that resource patchiness at the base of the aquatic microbial food web (dissolved nutrients, phytoplankton) could support the rapid development of patches at higher trophic levels (e.g., heterotrophic bacteria, phagotrophic flagellates), potentially driving a cascade of patch formation and exploitation. This cascade could, in turn, drive an accelerated rate of transfer of energy and matter from the inorganic nutrient pool through the microbial loop to the higher marine food web. In light of the highly specialized and diverse behavioral responses to spatially heterogeneous resources observed here, we propose that many microbial interactions in the ocean probably occur in such a patchy scenario, as opposed to the homogeneous "bulk phase" often employed in model marine systems.

## Acknowledgments

We are grateful to T. Ahmed for assistance with microfluidic fabrication and to H. Jang for preparing the schematic in figure 1. We thank D. Grünbaum and T. Kiørboe for helpful advice on the research and T. Ahmed, M. Durham, B. Kirkup, S. Menden-Deuer, J. G. Mitchell, and two anonymous reviewers for insightful and constructive comments on an earlier version of this manuscript. This research was funded by National Science Foundation grant OCE-0526241.

## APPENDIX

## Numerical Models

### *Individual-Based Model*

An individual-based model was designed with the objective of validating that the measured swimming parameters observed here will lead to accumulation of cells within the center of the nutrient patch, as was observed in the ex-

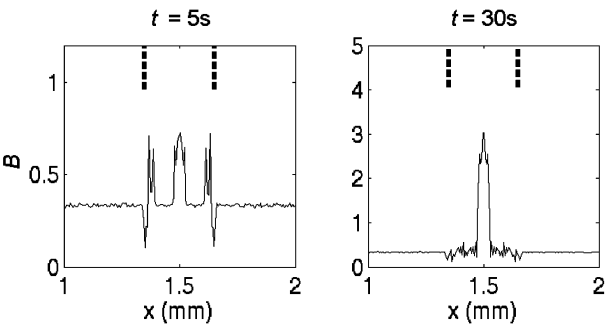


**Figure A1:** Cell distribution ($B$ = the cell concentration normalized by the total number of cells) predicted by the individual-based model at time $t = 5$ s (*left*) and $t = 30$ s (*right*). The dashed lines indicate the edges of the patch.

periments. In the model, a total of $10^6$ cells were tracked over 120 s in a one-dimensional domain (direction $x$) of width $W = 3$ mm (the channel width), corresponding to the transverse direction in the microchannel. The swimming behaviors ($u$, $f$) were taken to reflect experimental observations. Here we describe the case of *Dunaliella tertiolecta*, where cells swam at a constant speed $u = 38$ $\mu$m $s^{-1}$ and had a higher turning frequency $f = 2.0$ $s^{-1}$ outside a 300-$\mu$m-wide central region (the patch) and a lower turning frequency $f = 1.4$ $s^{-1}$ inside that region. To simulate chemotaxis, the turning frequency $f$ was biased by a fractional component, either $-\Delta$ or $+\Delta$, when swimming toward or away from the center ($x = W/2$) of the patch, respectively; that is, the turning frequency was $(1 - \Delta)f$ when swimming toward the center and $(1 + \Delta)f$ when swimming away from it. A magnitude of $\Delta = 0.15$ was used, which is consistent with the measured value of the chemotactic velocity (14%) of *D. teritolecta* in our experiments. Note that, in this case, no attempt was made to correlate chemotaxis with concentration gradients (this was done in the continuum model described below). The cells were initially distributed uniformly over the domain, with a velocity direction chosen randomly among the $+x$ or $-x$ directions. A reflecting boundary condition was imposed at the two channel sidewalls ($x = 0$ and $x = W$). Cells were individually tracked over time in Matlab using a time step of $dt = 0.05$ s. Convergence was tested by varying the number of cells $N$ (from $3 \times 10^4$ to $1 \times 10^6$) and the time step $dt$ (from 0.025 to 0.1 s); differences among the results were negligible.

The output of the model consisted of the distribution of cells over the width of the channel. When values corresponding to the experimental measurements were applied, the population exhibited a rapid net migration into the center of the patch (fig. A1). Although accumulation of cells initially developed at the edges of the patch, the chemotactic migration of cells toward the center of the patch resulted in a single peak in cell concentration at the center of the domain within 30 s, paralleling what we observed in our experiments. When the model was run for parameters measured for *Pseudoalteromonas haloplanktis* ($f = 5.5$ $s^{-1}$ inside and $f = 8.0$ $s^{-1}$ outside the patch; $u = 70$ $\mu$m $s^{-1}$ inside and $u = 57$ $\mu$m $s^{-1}$ outside the patch), identical patterns to those observed for *D. tertiolecta*, that is, accumulation in the center of the patch, were obtained.

Interestingly, the model generated different results when chemotactic behavior was omitted from the simulation (i.e., $\Delta = 0$). In this instance, cells accumulated at the edges of the patch (fig. A2). This pattern occurred because the turning frequency $f$ was lower inside the patch and isotropic, unlike the previous case, leading to a higher diffusivity of the population of cells $D = u^2/f$ in this region. Consequently, cells accumulated at the patch edges. This pattern confirms the importance of chemotaxis, which biases the turning frequency of cells depending on whether they are swimming toward or away from the center of the patch, resulting in a net migration of the population toward the highest nutrient region at the center of the patch.

### *The Continuum Model*

A continuum model was developed to predict the evolution, in time $t$ and space $x$, of the concentration $B(x, t)$ of a population of organisms as a result of random motility (swimming in the absence of chemical cues) and chemotaxis (directed motion up a chemoattractant gradient). The model—sometimes referred to as the cell transport equation—consisted of the partial differential equation

$$\frac{\partial B}{\partial t} = \frac{\partial}{\partial x}\left(\mu \frac{\partial B}{\partial x}\right) - \frac{\partial}{\partial x}(v_c B), \tag{A1}$$

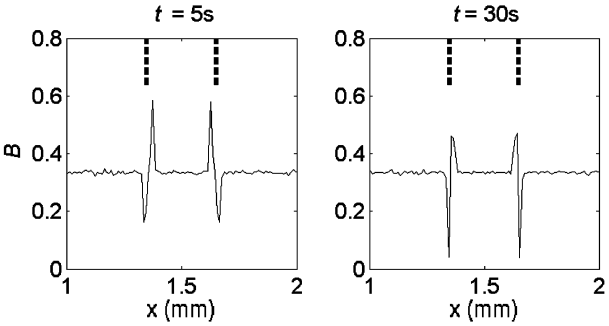


**Figure A2:** As in figure A1, but in the absence of chemotaxis.

which describes the rate of change of the concentration of cells $\partial B/\partial t$ resulting from random motility (first term on the right-hand side) and chemotaxis (last term). A continuum description is applicable here because the run length of the organisms ($u/f \sim$ 19–27 $\mu$m for *D. tertiolecta*; ~7–13 $\mu$m for *P. haloplanktis*) is always much smaller than the length scale of the patch (>300 $\mu$m).

Random motility is a diffusive process, which tends to homogenize the distribution of cells. The associated diffusivity $\mu$, called the random motility coefficient, scales as $\mu \sim u^2/f$. We used values of $u$ and $f$ observed in our experiments to determine the random motility inside ($\mu_{in}$) and outside ($\mu_{out}$) the central $L = 300$-$\mu$m-wide region (the patch). Random motility was then prescribed as a spatially varying function $\mu(x) = \mu_{out} + 0.5(\mu_{out} - \mu_{in})\{\tanh[(x + L/2)/\delta] - \tanh[(x - L/2)/\delta]\}$, expressing a transition from a constant $\mu_{out}$ to a constant $\mu_{in}$ over a distance $\delta = 50$ $\mu$m in the simulations, to mimic a sharp transition.

Chemotaxis, on the other hand, allows cells to drift toward higher resource (or "chemoattractant") concentrations and thus accumulate in those regions. The chemotactic velocity $v_c$ represents the mean speed at which the population migrates up chemoattractant gradient, and it depends on the magnitude of the chemoattractant gradient itself. We therefore also need to predict the chemoattractant concentration $C(x, t)$. To do so, we coupled equation (A1) with the diffusion equation for $C(x, t)$:

$$\frac{\partial C}{\partial t} = D_C \frac{\partial^2 C}{\partial x^2}, \tag{A2}$$

where $D_C$ is the molecular diffusivity of the chemoattractant ($D_C = 10^{-9}$ m$^2$ s$^{-1}$ for most low-molecular-weight compounds). The dependence of the chemotactic velocity on the chemoattractant concentration gradient $G$ (where $G = \partial C/\partial x$) was assumed to obey a saturation relation of the form $v_c = v_{c,max}G/(|G| + G_S)$, which expresses a linear increase of $v_c$ for small concentration gradients and a saturation for gradients larger than a threshold (or half-saturation) gradient $G_S$. The maximum chemotactic velocity $v_{c,max}$ was estimated from the experiments. The concentration gradient $G$ was obtained from equation (A2) and, in the absence of more detailed physiological information about the chemotaxis systems of the organisms at hand, $G_S$ was treated as a fitting parameter.

For both equations (A1) and (A2), a no-flux boundary condition was implemented at the two sidewalls ($x = 0$ and $x = W$) of a $W = 3$-mm-wide domain, corresponding to the microchannel width. The model was implemented in dimensionless form by nondimensionalizing the concentration of cells $B$ by its initial, uniform value (such that $B(x, 0) = 1$) and the concentration of chemoattractants $C$ by its maximum initial concentration. The initial concentration profile was taken to be a gaussian ($C(x, 0) = \exp[-x^2/\sigma^2]$) of width $\sigma = L/2 = 150$ $\mu$m (as in the experiments). The model (eqq. [A1], [A2]) was solved using finite element software (Comsol) with 960 elements. Convergence was tested by repeating simulations with twice the number of elements; differences in the results were found to be negligible. The outcome of the model consisted in the spatiotemporal evolution of $C(x, t)$ and $B(x, t)$.

A wide range of parameter values was explored. In the manuscript, we present two spatiotemporal maps of $B(x, t)$ for parameter values corresponding to the observations made for *D. tertiolecta* and *P. haloplanktis*. For *D. tertiolecta*, we used $\mu_{out} = 7.2 \times 10^{-10}$ m$^2$ s$^{-1}$ (corresponding to $f = 2.0$ s$^{-1}$ and $u = 38$ $\mu$m s$^{-1}$ measured outside the patch), $\mu_{in} = 10.2 \times 10^{-10}$ m$^2$ s$^{-1}$ (corresponding to $f = 1.4$ s$^{-1}$ and $u = 38$ $\mu$m s$^{-1}$ measured inside the patch), and $v_{c,max} = 5.3$ $\mu$m s$^{-1}$ $= 0.14u$. For *P. haloplanktis*, we used $\mu_{out} = 3.9 \times 10^{-10}$ m$^2$ s$^{-1}$ (corresponding to $f = 8.0$ s$^{-1}$ and $u = 57$ $\mu$m s$^{-1}$ measured outside the patch), $\mu_{in} = 9.0 \times 10^{-10}$ m$^2$ s$^{-1}$ (corresponding to $f = 5.5$ s$^{-1}$ and $u = 70$ $\mu$m s$^{-1}$ measured inside the patch), and $v_{c,max} = 5.0$ $\mu$m s$^{-1}$ $= 0.09u$. For both cases, $G_S = 0.04$ mm$^{-1}$.

## Literature Cited


Adler, J. 1969. Chemoreceptors in bacteria. Science 166:1588–1597.

Azam, F. 1998. Microbial control of oceanic carbon flux: the plot thickens. Science 280:694–696.

Azam, F., and J. W. Ammerman. 1984. Cycling of organic matter by bacterioplankton in pelagic marine ecosystems: microenvironmental considerations. Pages 345–360 *in* M. J. R. Fasham, ed. Flows of energy and materials in marine ecosystems. Plenum, New York.

Azam, F., and R. E. Hodson. 1981. Mutliphasic kinetics for D-glucose uptake by assemblages of natural marine bacteria. Marine Ecology Progress Series 6:213.

Azam, F., and R. A. Long. 2001. Sea snow microcosms. Nature 414: 495–498.

Azam, F., and F. Malfatti. 2007. Microbial structuring of marine ecosystems. Nature Reviews Microbiology 5:782–791.

Azam, F., T. Fenchel, J. G. Field, J. S. Gray, L. A. Meyer-Reil, and F. Thingstad. 1983. The ecological role of water-column microbes in the sea. Marine Ecology Progress Series 10:257–263.

Barbara, G. M., and J. G. Mitchell. 2003*a*. Bacterial tracking of motile algae. FEMS Microbiology Ecology 44:79–87.

———. 2003*b*. Marine bacterial organisation around point-like sources of amino acids. FEMS Microbiology Ecology 43:99–109.

Bell, W., and R. Mitchell. 1972. Chemotactic and growth responses of marine bacteria to algal extracellular products. Biology Bulletin 143:265–277.

Benhamou, S. 1992. Efficiency of area-concentrated searching behavior in a continuous patchy environment. Journal of Theoretical Biology 159:67–81.

Berg, H. C. 1993. Random walks in biology. Princeton University Press, Princeton, NJ.

Berg, H. C., and D. A. Brown. 1972. Chemotaxis in *Escherichia coli* analysed by three-dimensional tracking. Nature 239:500–504.

Blackburn, N., and T. Fenchel. 1999*a*. Influence of bacteria, diffusion and shear on micro-scale nutrient patches, and implications for bacterial chemotaxis. Marine Ecology Progress Series 189:1–7.

———. 1999*b*. Modelling of microscale patch encounter by chemotactic protozoa. Protist 150:337–343.

Blackburn, N., F. Azam, and Å. Hagström. 1997. Spatially explicit simulations of a microbial food web. Limnology and Oceanography 42:613–622.

Blackburn, N., T. Fenchel, and J. G. Mitchell. 1998. Microscale nutrient patches in plankton habitats shown by chemotactic bacteria. Science 282:2254–2256.

Bowen, J. D., K. D. Stolzenbach, and S. W. Chisholm. 1993. Simulating bacterial clustering around phytoplankton cells in a turbulent ocean. Limnology and Oceanography 38:36–51.

Brentnall, S. J., K. J. Richards, J. Brindley, and E. Murphy. 2003. Plankton patchiness and its effect on larger-scale productivity. Journal of Plankton Research 25:121–140.

Brown, D. A., and H. C. Berg. 1974. Temporal stimulation of chemotaxis in *Escherichia coli*. Proceedings of the National Academy of Sciences of the USA 71:1388–1392.

Buskey, E. J. 1984. Swimming pattern as an indicator of the roles of copepod sensory systems in the recognition of food. Marine Biology 79:165–175.

Cole, J. J. 1982. Interactions between bacteria and algae in aquatic ecosystems. Annual Review of Ecological Systems 13:291–314.

Crenshaw, H. C. 1993. Orientation by helical motion. III. Microorganisms can orient to stimuli by changing the direction of their rotational velocity. Bulletin of Mathematical Biology 55:231–255.

———. 1996. A new look at locomotion in microorganisms: rotating and translating. American Zoologist 36:608–618.

Dahlquist, F. W., R. A. Elwell, and P. S. Lovely. 1976. Studies of bacterial chemotaxis in defined concentration gradients: model for chemotaxis towards L-serine. Journal of Supramolecular Structure 4:329–342.

D'Orsogna, M. R., M. A. Suchard, and T. Chou. 2003. Interplay of chemotaxis and chemokinesis mechanisms in bacterial dynamics. Physical Review E68:021925.

Doubell, M. J., L. Seuront, J. R. Seymour, N. L Patten, and J. G. Mitchell. 2006. High-resolution fluorometer for mapping microscale phytoplankton distributions. Applied and Environmental Microbiology 76:4475–4478.

Erga, S. R., M. Dybwad, O. Frette, J. K. Lotsberg, and K. Aursland. 2003. New aspects of migratory behaviour of phytoplankton in stratified waters: effects of halocline strength and light on *Tetraselmis* sp. (Prasinophyceae) in an artificial water colum. Limnology and Oceanography 48:1202–1213.

Fenchel, T. 2002. Microbial behaviour in a heterogenous world. Science 296:1068–1071.

Fenchel, T., and N. Blackburn. 1999. Motile chemosensory behaviour of phagotrophic protists: mechanisms for and efficiency in congregating at food patches. Protist 150:325–336.

Fenchel, T., and P. R. Jonsson. 1988. The functional biology of *Strombidium sulcatum*, a marine oligotrich ciliate (Ciliophira, Oligotrichnia). Marine Ecology Progress Series 48:1–15.

Gao, Q., M. Yu, J. Wang, H. Jia, and K. Wang. 2004. Relationships between regional primary production and vegetation patterns. Ecological Modelling 172:1–12.

Goldman, J. C., and P. M. Gilbert. 1982. Comparative rapid ammonium uptake by four species of marine phytoplankton. Limnology and Oceanography 27:814–827.

Goldman, J. C., J. J. McCarthy, and D. G. Peavey. 1979. Growth rate influence on the chemical composition of phytoplankton in oceanic waters. Nature 279:210–215.

Govoronova, E. G., and O. A. Sineshchekov. 2005. Chemotaxis in the green flagellate alga *Chlamydomonas*. Biogeochemistry 70:717–725.

Grünbaum, D. 1998. Using spatially explicit models to characterize foraging performance in heterogeneous landscapes. American Naturalist 151:97–115.

Guillard, R. R. L., and J. H. Ryther. 1962. Studies of marine planktonic diatoms. I. *Cyclotella nana* Hustedt and *Detonula confervacea* Cleve. Canadian Journal of Microbiology 8:229–239.

Haury, L. R., J. A. McGowan, and P. H. Wiebe. 1978. Patterns and processes in the time-space scales of plankton distributions. Pages 277–328 *in* J. H. Steele, ed. Spatial pattern in plankton communities. Plenum, New York.

Horner, R. A., D. L. Garrison, and F. G. Plumley. 1997. Harmful algal blooms and red tide problems on the US west coast. Limnology and Oceanography 42:1076–1088.

Hutchinson, G. E. 1961. The paradox of the plankton. American Naturalist 95:137–145.

Jackson, G. A. 1980. Phytoplankton growth and zooplankton grazing in oligotrophic oceans. Nature 284:439–441.

———. 1987. Simulating chemosensory responses of marine microorganisms. Limnology and Oceanography 32:1253–1266.

Johansen, J. E., J. Pinhassi, N. Blackburn, U. L. Zweifel, and A. Hagström. 2002. Variability in motility characteristics among marine bacteria. Aquatic Microbial Ecology 28:229–237.

Kamykowski, D., E. J. Milligan, and R. E. Reed. 1998. Relationships between geotaxis/phototaxis and diel vertical migration in autotrophic dinoflagellates. Journal of Plankton Research 20:1781–1796.

Keymer, J. E., P. Galajda, C. Muldoon, S. Park, and R. H. Austin. 2006. Bacterial metapopulations in nanofabricated landscapes. Proceedings of the National Academy of Sciences of the USA 103:17290–17295.

Kiørboe, T., and G. A. Jackson. 2001. Marine snow, organic solute plumes, and optimal chemosensory behaviour of bacteria. Limnology and Oceanography 46:1309–1318.

Kohidai, L., P. Kovacs, and G. Csaba. 1996. Chemotaxis of the unicellular green alga *Dunaliella salina* and the ciliated *Tetrhymena pyriformis*: effects of glycine, lysine, and alanine and their oligopeptides. Bioscience Reports 16:467–476.

Lazier, J. R. N., and K. H. Mann. 1989. Turbulence and the diffusive layers around small organisms. Deep Sea Research 36:1721–1733.

Lee, E. S., A. J. Lewitus, and R. K. Zimmer. 1999. Chemoreception in a marine cryptophyte: behavioural plasticity in response to amino acids and nitrate. Limnology and Oceanography 44:1571–1574.

Lee, W. J., A. G. B. Simpson, and D. J. Patterson. 2005. Free-living heterotrophic flagellates from freshwater sites in Tasmania (Australia), a field survey. Acta Protozoology 44:321–350.

Lehman, J. T., and D. Scavia. 1982*a*. Microscale nutrient patches produced by zooplankton. Proceedings of the National Academy of Sciences of the USA 79:5001–5005.

———. 1982*b*. Microscale patchiness of nutrients in plankton communities. Science 216:729–730.

Leising, A. W. 2001. Copepod foraging in patchy habitats and thin

layers using a 2-D individual based model. Marine Ecology Progress Series 216:167–179.

Leising, A. W., and P. J. S. Franks. 2000. Copepod vertical distribution within a spatially variable food source: a simple foraging-strategy model. Journal of Plankton Research 22:999–1024.

———. 2002. Does *Acartia clausi* (Copepoda: Calanoida) use an area-restricted search foraging strategy to find food? Hydrobiologia 480:193–207.

Levin, S. A., and M. Whitfield. 1994. Patchiness in marine and terrestrial systems: from individuals to populations. Philosophical Transactions of the Royal Society B: Biological Sciences 343:99–103.

Lovely, P. S., and F. W. Dahlquist. 1975. Statistical measures of bacterial motility and chemotaxis. Journal of Theoretical Biology 50: 477–496.

Mao, H., P. S. Crèmer, and M. D. Manson. 2003. A sensitive, versatile microfluidic assay for bacterial chemotaxis. Proceedings of the National Academy of Sciences of the USA 100:5449–5454.

Marcos and R. Stocker. 2006 Microorganisms in vortices: a microfluidic setup. Limnology and Oceanography Methods 4:392–398.

McCarthy, J. J., and J. C. Goldman. 1979. Nitrogenous nutrition of marine phytoplankton in nutrient depleted waters. Science 203: 670–672.

Menden-Deuer, S., and D. Grünbaum. 2006. Individual foraging behaviors and population distributions of a planktonic predator aggregating to phytoplankton thin layers. Limnology and Oceanography 51:109–116.

Mitchell, J. G. 1991. The influence of cell size on marine bacterial motility and energetics. Microbial Ecology 22:227–238.

Mitchell, J. G., A. Okubo, and J. A. Fuhrman. 1985. Microzones surrounding phytoplankton form the basis for a stratified marine microbial ecosystem. Nature 316:58–59.

Mitchell, J. G., L. Pearson, A. Bonazinga, S. Dillon, H. Khouri, and R. Paxinos. 1995. Long lag times and high velocities in the motility of natural assemblages of marine bacteria. Applied and Environmental Microbiology 61:877–882.

Mitchell, J. G., L. Pearson, and S. Dillon. 1996. Clustering of marine bacteria in seawater enrichments. Applied and Environmental Microbiology 62:3716–3721.

Mittal, N., E. O. Budrene, M. P. Brenner, and A. van Oudenaarden. 2003. Motility of *Escherichia coli* cells in clusters formed by chemotactic aggregation. Proceedings of the National Academy of Sciences of the USA 100:13259–13263.

Moran, M. A., A. Buchan, J. M. González, J. F. Heidelberg, W. B. Whitman, R. P. Kiene, J. R. Henriksen, et al. 2004. Genome sequence of *Silicibacter pomeroyi* reveals adaptations to the marine environment. Nature 432:910–913.

Mullin, M. M., and E. R. Brooks. 1976. Some consequences of distributional heterogeneity of phytoplankton and zooplankton. Limnology and Oceanography 21:784–796.

Nachman, G. 2006. A functional response model of a predator population foraging in a patchy habitat. Journal of Animal Ecology 75:948–958.

Packer, H. L., and J. P. Armitage. 1994. The chemokinetic and chemotactic behaviour of *Rhodobacter sphaeroides*: two independent responses. Journal of Bacteriology 176:206–212.

Park, S., P. M. Wolanin, E. A. Yuzbahyan, H. Lin, N. C. Darnton, J. B. Stock, P. Silberzan, and R. Austin. 2003. Influence of topology on bacterial social interaction. Proceedings of the National Academy of Sciences of the USA 100:13910–13915.

Prezelin, B. B., and A. L. Alldredge. 1983. Primary production of marine snow during and after an upwelling event. Limnology and Oceanography 28:1156–1167.

Rivero, M. A., R. T. Tranquillo, H. M. Buettner, and D. A. Lauffenburger. 1989. Transport models for chemotactic cell populations based on individual cell behaviour. Chemical Engineering Science 44:2881–2897.

Rothschild, B. J., P. J. Haley, and D. Cai. 1999. Influence of physical forcing on microclouds of dissolved organic matter and nutrients in the ocean. Journal of Plankton Research 21:1217–1230.

Rovinsky, A. B., H. Adiwidjaja, V. Z. Yaknio, and M. Menzinger. 1997. Patchiness and enhancement of productivity in plankton ecosystems due to the differential advection of predator and prey. Oikos 78:101–106.

Schoevaert, D., S. Krishnaswamy, M. Couturier, and F. Marano. 1988. Ciliary beat and cell motility of *Dunaliella*: computer analysis of high speed microcinematography. Biology of the Cell 62:229–240.

Seymour, J. R., J. G. Mitchell, L. Pearson, and R. Waters. 2000. Heterogeneity in bacterioplankton abundance from 4.5 millimetre resolution sampling. Aquatic Microbial Ecology 22:143–153.

Seymour, J. R., J. G. Mitchell, and L. Seuront. 2004. Microscale heterogeneity in the activity of coastal bacterioplankton communities. Aquatic Microbial Ecology 35:1–16.

Seymour, J. R., Marcos, and R. Stocker. 2007. Chemotactic response of marine micro-organisms to microscale nutrient layers. Journal of Visualized Experiments 4. http://www.jove.com/index/details.stp?id=203.

Sherr, E. B., and B. F. Sherr. 2002. Significance of predation by protists in aquatic food webs. Antonie van Leeuwenhoek 81:293–308.

Sibbald, M. J., L. J. Albright, and P. R. Sibbald. 1987. Chemosensory response of a heterotrophic microflagellate to bacteria and several nitrogen compounds. Marine Ecology Progress Series 36:201–204.

Sjoblad, R. D., and P. H. Frederikse. 1981. Chemotactic response of *Chlamydomonas reinhardtii*. Molecular and Cellular Biology 1: 1057–1060.

Stocker, R., J. R. Seymour, A. Samadani, D. H. Hunt, and M. Polz. 2008. Rapid chemotactic response enables marine bacteria to exploit ephemeral microscale nutrient patches. Proceedings of the National Academy of Sciences of the USA 105:4209–4214.

Thar, R., and T. Fenchel. 2005. Survey of motile microaerophilic bacterial morphotypes in the oxygen gradient above a marine sulfidic sediment. Applied and Environmental Microbiology 71:3682–3691.

Tiselius, P. 1992. Behaviour of *Arcatia tonsa* in patchy food environments. Limnology and Oceanography 37:1640–1651.

Weibel, D. B., W. R. DiLuzio, and G. M. Whitesides. 2007. Microfabrication meets microbiology. Nature Reviews Microbiology 5: 209–218.

Whitesides, G. M., E. Ostuni, S. Takayama, X. Jiang, and D. E. Ingber. 2001. Soft lithography in biology and biochemistry. Annual Review of Biomedical Engineering 3:335–373.

Wiens, J. A. 1989. Spatial scaling in ecology. Functional Ecology 3: 385–397.

Williams, P. J., and L. R. Muir. 1981. Diffusion as a constraint on the biological importance of microzones in the sea. Pages 209–218 *in* J. C. J. Nihoul, ed. Ecohydrodynamics. Elsevier, Amsterdam.

Zhulin, I. B., and J. P. Armitage. 1993. Motility, chemokinesis and methylation-independent chemotaxis in *Azospirillum brasilenese*. Journal of Bacteriology 175:952–958.

Associate Editor: Daniel L. Roelke
Editor: Donald L. DeAngelis